Effect of extending conjugation via thiophene-based oligomers on the excited state electron transfer rates to ZnO nanocrystals

Effect of Extending Conjugation via Thiophene-Based Oligomers on the Excited State Electron Transfer Rates to ZnO Nanocrystals

Amanda N. Oehrlein[†], Antonio Sanchez-Diaz[†], Philip C. Goff[†], Miquel Planells[§], Neil Robertson[§], David A. Blank[†*], Wayne L. Gladfelter[†*]

[†]*Department of Chemistry, University of Minnesota- Twin Cities, Minneapolis, MN 55455-0431*

[‡]*Department of Chemistry, University of Minnesota- Morris, Morris, MN 56267*

[§]*EastChem School of Chemistry, University of Edinburgh West Mains Road, Edinburgh EH9 3JJ, U.K.*

Corresponding Authors
Wayne L. Gladfelter wlg@umn.edu, David A. Blank blank@umn.edu

Abstract

Oligothiophene dyes with two to five thiophene units were anchored to oleate-capped, quantum-confined zinc oxide nanocrystals (ZnO NCs) through a cyanoacrylate functional group. While the fluorescence of the bithiophene derivative was too weak for meaningful quenching studies, the fluorescence of the dyes with three, four and five thiophene rings was quenched upon binding to the NCs. Ultrafast pump-probe spectroscopy was used to observe the singlet excited states of the free dyes dissolved in dichloromethane as well as attached to a ZnO NC dispersed in the same solvent. When the dyes were bound to ZnO NCs, ultrafast spectroscopic measurements revealed rapid disappearance of the singlet excited state and appearance of a new transient absorption at higher energy that was assigned to the oxidized dye based on the similar absorption observed upon oxidation of the dye using nitrosonium ion. The appearance lifetimes of the oxidized dyes were

assigned to the excited state electron transfer and were 36 ± 2, 22.3 ± 3.9, 26.5 ± 1.5 and 19.4 ± 0.8 ps for bi-, ter-, quarter- and quinquethiophene dyes respectively. Two factors contributed to the similarity in the electron transfer lifetime. First the excited state energies of the dyes were similar, and second, the free energy for electron transfer reaction was sufficiently large to move the event into the energy-independent regime.

Keywords: Dye sensitized solar cells, zinc oxide nanocrystals, ultrafast transient absorption spectroscopy, excited state electron transfer

Introduction

Monodisperse zinc oxide nanocrystals (NCs) have been shown to serve as a useful platform for studying light-induced charge separation as found in dye-sensitized solar cells. Using a variety of dyes, including porphyrins,[1] ruthenium tris(bipyridine) complexes[2] and terthiophenes,[3-5] our past work has addressed the impact of dye structure, excited state energy of the dye, anchoring group and ZnO NC diameter on the excited state electron transfer lifetime. Thiophene oligomers offer the ability to tune the dye absorption through systematic extension of the oligomer chain, and associated conjugation, with the potential to cover the entire visible spectrum within a chemically homologous series. The ability to cover a broad range of the spectrum is advantageous in the context of light harvesting, but the question that immediately arises in the context of a dye sensitized photovoltaic is how the extension in conjugation influences the rate of electron transfer. One factor is the donor-acceptor energetic alignment. However, changes in the absorption energy in the thiophene oligomer series are dominated by increases in the HOMO energy with length[6] and this suggests that energetic alignment between the excited donor and the ZnO accepter should

remain largely unaffected. Another factor is the donor-acceptor distance.[7-9] In a series of thiophene oligomers, as the oligomer chain is extended one might expect a decrease in the donor acceptor coupling as the average distance increases, with an associated reduction in the electron transfer rate. A prior study on TiO_2 adjusted the donor acceptor distance through extension of a conjugated bridge, however this had only a minor influence on the absorption spectrum and the electron injection rate was not resolved.[10] The hypotheses investigated in this report is that a series of thiophene oligomer dyes can be used to cover the visible spectrum while maintaining rapid, efficient electron transfer by mitigating the systematic increase in donor-acceptor distance with an electron withdrawing linker that localizes the excited state near the donor-acceptor interface. Recent reports have established cyanoacrylates as effective dye terminating groups in dye-sensitized solar cells.[11-14] In addition to the carboxylic acid functional group serving as the anchor to metal oxide surface, the entire cyanoacrylate moiety is a powerful electron acceptor, which reduces the HOMO-LUMO gap and localizes the excited state electron density in close proximity to the metal oxide surface.[6, 14, 15]

In this study, we bound a series of oligothiophene dyes to ZnO NCs through a cyanoacrylate anchoring group (Figure 1) and measured their excited state electron transfer rates using ultrafast pump-probe spectroscopy. Compounds **3T** and **4T** are known to be effective interface modifiers in dye-sensitized solar cells,[6, 16] and **5T** itself has been demonstrated an effective dye for solar cells.[17, 18] This series of compounds is of particular interest because, despite large differences in their absorption spectra, the energies of the LUMOs, which are primarily localized on the cyanoacrylate moiety and the adjacent thiophene ring, of **2T**, **3T**, **4T** and **5T** were reported to be similar.[6] As such, rate measurement of excited state electron transfer could reveal whether or not the rates are independent of the chromophore structure past the anchoring group and the first

thiophene. Such behavior could conceivable allow one to tune and expand the light harvesting bandwidth of a solar cell using multiple dyes with minimal problems resulting from substantially different excited state electron transfer rates.

Experimental

General Information. Dimethyl sulfoxide (DMSO), absolute ethanol, zinc acetate ($Zn(CH_3COO)_2•2H_2O$), tetramethylammonium hydroxide ($[Me_4N]OH•5H_2O$) ethyl acetate, dichloromethane, dimethylformamide were used without purification from Sigma Aldrich. Methanol (VWR) was used for dispersing the nanocrystal solutions. UV-Vis absorption spectra were obtained using a Cary 14 spectrophotometer or an Ocean Optics USB 2000 spectrometer with a tungsten and deuterium light source. The steady state emission spectra were collected using a Varian Cary Eclipse Fluorescence Spectrophotometer with a right angle set up or a Spex Fluorolog 1680 0.22 m double spectrometer equipped with a xenon source. All spectroscopy was performed under argon or air using 1 cm quartz cuvettes. The presence of air did not quench the fluorescence. Fluorescence spectra were compensated for changes in the instrument's sensitivity at longer wavelengths. The synthesis and characterization of **2T**, **3T**, **4T**, and **5T** have been published elsewhere.[6] Figure 2 shows the electronic adsorption and fluorescence spectra of the dyes in dichloromethane solution.

ZnO Nanocrystal Synthesis. The synthesis of ZnO NCs was adapted from Gamelin and co-workers.[19] A 0.55 M solution of $[Me_4N]OH•5H_2O$ in absolute ethanol (7.7 mL, 4.25 mmol) was added dropwise into a 0.1 M solution of $Zn(CH_3COO)_2•2H_2O$ in dimethylsulfoxide (25 mL, 2.51 mmol) over 8 min and allowed to stir at 40°C for 25 min. The nanocrystals were purified by precipitation with ethyl acetate (~9 mL) and isolated after centrifugation. To cap the ZnO NCs

with oleate groups, the NCs from the above preparation were combined with 5 mL of a 12.7 mM solution of oleic acid in CH_2Cl_2 and sonicated. The capped NCs were precipitated with 9 mL of absolute ethanol and the mixture centrifuged. After removal of the supernatant, CH_2Cl_2 was added (10 mL) and the mixture was sonicated.

The onset of absorption in the UV region was used to measure the NC diameter. The oleic acid-capped NCs had diameters of 4.3 nm. Nanocrystal concentrations were estimated assuming full conversion of starting material and were used within 24 hours of synthesis.

Quenching Experiments. For **3T** and **4T**, samples were prepared in CH_2Cl_2 using varying aliquots (37 μL to 5.5 mL of a 2.28×10^{-5} M ZnO NC dispersion) and a sufficient volume of a stock dye solution to bring the final dye concentration to 1.80×10^{-5} M following dilution to the total sample volume of 7.0 mL. This generated a range of dye-to-ZnO NC ratios of ~150:1 to 1:1. For **5T**, samples were prepared in CH_2Cl_2 using varying aliquots (33 μL to 3.28 mL of a 1.92×10^{-5} M ZnO NC dispersion) and a sufficient volume of a stock dye solution to bring the final dye concentration to 1.80×10^{-5} M following dilution to the total sample volume of 7.0 mL. This generated a range of dye-to-ZnO NC ratios of ~200:1 to 2:1. For comparison, one solution of each dye was deprotonated by adding 10 μL of a 0.1 M $[Me_4N]OH$ solution in CH_3OH to a dye solution followed by dilution to 10 mL with CH_2Cl_2. Electronic absorption and fluorescence spectra of each sample were measured. Stern Volmer graphs were made by dividing the fluorescence of the dye alone solution (I_o) by the fluorescence of the dye plus ZnO NC solution (I) and plotting the result vs the ZnO NC concentration.

Chemical Oxidation of the Dyes. Solutions of each dye were prepared by diluting a 1.0 mL aliquot of a 1.8×10^{-5} M solution to a final volume of 10.0 mL with CH_2Cl_2. To 3 mL of this solution of dye was added 8 mg of solid $[NO][PF_6]$. For **2T** 8 mg of $[NO][SbF_6]$ was used in place

of [NO][PF_6] because the latter did not oxidize the dye. UV-vis spectra were taken before and 30 s after addition of the oxidant. The spectra measured following the addition of oxidant showed absorption bands from both the starting dyes and their oxidized products.

Fluorescence Lifetimes and Quantum Yields. Fluorescence lifetimes longer than 500 ps were measured using time-correlated single photon counting. The experimental setup has been reported previously.[20] Samples in a 1 cm quartz cell were excited using a 40 MHz diode laser (Picoquant LDH-P-C-375) at 375 nm and 40 MHz diode laser (Picoquant LDH-P-C-470) at 470 nm. Sample emission was detected using an avalanche photodiode at a right-angle geometry at the exit of a double monochromator (Jobin-Yvon TRIAX-320). Fluorescence quantum yields, Φ_F, were calculated using the simple point method employing Rhodamine 6G as standard reference. All emission spectra were collected at 90º relative to the excitation light. Optical densities were less than 0.2, and all solutions were de-aerated with argon for 5 minutes before the spectrum was recorded.

Solutions for Pump-Probe Experiments. All dye-alone solutions used for the ultrafast measurements had a dye concentration of 1.8×10^{-5} M in CH_2Cl_2. Solutions comprising dye:ZnO NCs of 2:1 were prepared using the following mixtures that were ultimately diluted to 10.0 mL: **2T**:ZnO NC, 1.64 mL of a 1.10×10^{-4} M dye solution and 3.70 mL of a 2.44×10^{-5} M dispersion of ZnO NCs; **3T**:ZnO NC, 1.00 mL of a 1.8×10^{-4} M dye solution and 2.87 mL of a 3.12×10^{-5} M dispersion of ZnO NCs; **4T**:ZnO NCs, 1.97 mL of a 9.15×10^{-5} M dye solution and 3.70 mL of a 2.44×10^{-5} M dispersion of ZnO NCs; **5T**:ZnO NCs, 1.86 mL of a 9.71×10^{-5} M dye solution and 3.13 mL of a 2.92×10^{-5} M dispersion of ZnO NCs.

Frequency Resolved Pump-Probe Measurements. Details of the method were reported previously.[5] Briefly, the output of a home-built, amplified, Ti:sapphire based laser system

producing 100 fs, 0.5 mJ, 1.55 eV pulses at 1 kHz was split to create the pump and probe. The majority of the energy, 90%, was either frequency doubled in a BBO crystal or used to pump a home-built non-colinear OPA producing excitation pulses at 3.1 eV or in the range 1.8-2.6 eV, respectively. The remaining 10% of the energy at 1.55 eV was focused into a 2 mm thick sapphire window to create a continuum probe. The pump and probe were crossed in a 1 mm optical pathlength sample cell with suprasil quartz windows (Starna), and the samples were flowed through the sample cell at a rate of 35 ml/min. After the sample, the probe continuum was columnated, refocused into a monochromator (Princeton Instruments 2150), and dispersed onto a linear silicon diode array with 256 elements (Hamamatsu) providing an effective resolution of 2 nm. The probe spectrum was recoded for every laser pulse, while the pump was modulated at half the laser repetition rate using a mechanical chopper wheel. The difference in optical density, ΔOD, was determined for each pulse pair (pump on – pump off), and then averaged over 50,000 pulse pairs at each delay time. Pump pulse irradiance was typically 140 $\mu J/cm^2$. There was no change in the absorption spectrum before and after the pump-probe experiments, and thus no evidence of photodegradation. The instrument response was 80 fs (Gaussian, FWHM).

Results

In dichloromethane the electronic absorption spectra (Figure 2) of **2T**, **3T**, **4T**, and **5T** consisted of an intense peak at 2.92 (425), 2.73 (454), 2.64 (470), and 2.62 (473) eV (nm) and a weaker peak at 4.13 (300), 3.79 (327), 3.46 (358), and 3.23 (384) eV (nm), respectively. The fluorescence maxima for **2T**, **3T, 4T**, and **5T** occurred at 2.40 (517), 2.06 (602), 1.84 (674) and 1.74 (713) eV (nm), respectively.

Steady State Fluorescence Quenching with ZnO NCs. Stern-Volmer plots are shown in Figure 3 for **3T**, **4T**, and **5T** using ZnO NCs as the quencher (**2T** was not studied as the fluorescence was too weak). Each graph exhibited an initial linear region, which was consistent with static quenching, however, maximum quenching appeared as the dye:ZnO NC ratio approached ~20:1. Further quencher addition caused a decrease in emission until a plateau was reached at a dye:ZnO NC of approximately two. The general shape of the Stern Volmer graphs observed for these dyes paralleled those reported in earlier studies, where the suggested causes were concentration quenching[21] or competition between dye binding sites that were or were not quenched.[3, 4] The current work focused on the ultrafast quenching kinetics at a dye to ZnO NC of 2:1 in order to minimize any complications attributed to dye-dye interactions.

Oxidized Dye Generation. The strong, one-electron oxidant, nitrosonium ion, $[NO]^+$, either as the $[PF_6]^-$ or $[SbF_6]^-$ salt was used to oxidize the oligothiophene dyes in dichloromethane solution directly in a quartz cuvette. At room temperature the reaction was rapid, and the oxidization products had lifetimes on the order of minutes. In each case, a new absorption in the UV-visible region assigned to the oxidation product appeared at 2.4, 2.0, 1.8, and 1.7 eV for **2T**, **3T**, **4T**, and **5T**, respectively, and eventually decayed. The spectrum of the oxidized product was shown as a dashed, black line in Figure 4. The spectrum resulting from oxidation of **2T** also exhibited an unassigned peak at 1.70 eV.

Fluorescence Lifetimes and Quantum Yields for 3T, 4T and 5T. Time correlated single photon counting was used to measure the fluorescence lifetimes of **3T**, **4T** and **5T** in CH_2Cl_2. Each of the decay curves were well fit using a single exponential yielding fluorescence lifetimes of 760 ps (λ_{ex} = 2.64 eV, λ_{em} = 2.07 eV) for **3T**, 1560 ps (λ_{ex} = 2.64 eV, λ_{em} = 1.85 eV) for **4T** and 790 ps

(λ_{ex} = 2.64 eV, λ_{em} = 1.77 eV) for **5T**. The quantum yields for fluorescence were 0.15, 0.56 and 0.11 for **3T**, **4T** and **5T**, respectively.

Ultrafast Pump-Probe Spectroscopy. Pump-probe spectra were measured as the change in optical density, $\Delta OD(\lambda,t)$, induced by the pump excitation as a function of time delay between the pump and probe. The excitation wavelength was tuned to excite the lowest absorption band, and measurements were performed on **2T**, **3T**, **4T**, and **5T** with and without the presence of ZnO NCs in a CH_2Cl_2 solution. The dye to ZnO NC ratio was 2 to 1 for all ultrafast experiments.

2T. Figure 4A shows the observed spectra of **2T** at select time points following excitation at 3.10 eV. The transient absorption (TA) appeared within the time resolution of the experiment with a maximum intensity at 2.47 eV. This band overlapped both the stimulated emission (SE) at 2.25 eV and the ground state bleach (GB) at energies greater than 2.85 eV. After 100 ps the transient features decayed to the baseline indicating return to the ground state.

The pump-probe spectrum of a solution containing a 2:1 mixture of **2T** and ZnO NCs revealed a transient absorption at 2.35 eV (Figure 4B). The 0.1 eV red-shift relative to the free dye resulted from deprotonation and binding to the ZnO NC. As this feature decayed, a new feature centered at 2.44 eV formed and remained unchanged to the longest time measured (900 ps). Based on the similarity to the UV-vis spectrum of a chemically oxidized dye (dashed line in Figure 4B), the 2.44 eV TA was assigned to the oxidized dye that resulted from electron transfer to the ZnO NC.

3T. Figure 4C displays the pump-probe spectral changes at select time points for a solution of **3T** in CH_2Cl_2 following a 2.38 eV pump pulse. Immediately following excitation the difference spectrum exhibited a GB at 2.64 eV and a positive signal, due to the singlet excited state having a maximum intensity at 2.07 eV. As a function of time, a signal with maxima at 2.11 and 2.35 eV appeared and remained present to the longest time delay measured (900 ps)

Photolysis of a dichloromethane solution of **3T** in a 2:1 ratio with ZnO NCs ultimately led to a difference spectrum with a new maximum located at 2.03 eV. This was sufficiently close in energy to the oxidized dye (Figure 4D) to assign the peak to the product of excited state electron transfer. In addition to the peak at 2.03 eV, the GB no longer measurably decayed on the time scale of the experiment, indicating another process (i. e. oxidation of the dye) occurred to prevent recovery of the ground state during the lifetime of these measurements.

4T. Figure 4E shows the spectral evolution in the visible region of **4T** in CH_2Cl_2 upon 2.38 eV pump excitation. Two distinct temporal events were discernable from 0 - 900 ps coupled with a change that occurred on a time scale beyond the limit of the current experiments (> 900 ps). Between 0.25 and 10 ps the TA at 1.68 eV decreased, while a relatively smaller decrease was observed in the peak at 1.75 eV. As this occurred a new feature appeared at 2.2 eV. An isosbestic point at 1.95 eV is observable. In addition, during this same time regime, the GB minimum shifted from 2.66 to 2.70 eV. At delay times between 50 and 900 ps, there was a uniform decay of both the TA and GB signals, and a well-defined isosbestic point at 2.48 eV was visible.

Adsorption of **4T** on ZnO NCs resulted in a simplification of the spectral changes with time (Figure 4F). Unlike the dye-alone spectral changes, the two most intense TA peaks disappeared in unison as a new TA peaks emerges at 1.75 eV. The latter has the same energy as a sample of **4T** independently oxidized using $[NO][PF_6]$, allowing a confident assignment of this TA peak to the oxidized dye. The appearance of an imperfect isosbestic point at 1.72 eV was consistent with a relatively clean conversion from the singlet excited state of the bound dye to the product of electron transfer into the ZnO NC.

5T. Following a pump pulse at 2.38 eV, TA formed at 1.47 eV, and the feature seemed to stretch from the end of the detection range in the near IR (1.30 eV) to 1.66 eV (Figure 4G). Due

the interference of the residual light from the fundamental of the laser around 1.55 eV used to create the probe pulse, the absorption was interrupted, so the whole feature could not be studied. The signal did not return to the baseline by 900 ps. The ground state hole feature peaked at 2.55 eV and there was no stimulated emission for **5T**. There was also a broad feature centered around 2.07 eV.

In the dye and ZnO NC solution, a broad TA similar to the dye alone was initially seen. As this feature decayed, the emergence of another absorption appeared at 1.66 eV (Figure 4H). The absorption was attributed to the oxidized dye and matched well with chemical oxidation results (Figure 4H).

3T, 4T and 5T Fitting Procedure and Results. To analyze the electron transfer kinetics, we chose a probe energy in the dye alone transient absorption that had minimal time evolution over the first 200 ps of the experiment and then fit this, without ZnO NCs and with 2:1 ratio of dye to ZnO NCs. By selecting a probe energy that minimizes dynamics in the dye alone, any additional dynamics due to the presence of ZnO are well isolated. This approach provides a reasonably clean look at the electron transfer kinetics. The chosen energies were 2.07, 1.78 and 1.73 eV for **3T**, **4T** and **5T**, respectively. The dye alone signals fit well to an instantaneous appearance followed by a single exponential decay fixed to the time resolved emission data time constants of 760, 1560 and 790 ps for **3T**, **4T** and **5T**, respectively. This indicates that these probe energies have very little influence from any complicated solvation, relaxation, and other associated dynamics as a result of a confluence of overlapping signals in the spectral shifting, leaving only the lifetime in the time dependence.

When fitting the spectral changes of solutions containing a 2:1 ratio of dye to ZnO NCs at these same probe energies, there was the same initial instantaneous jump with the creation of the excited

state, and then a subsequent single exponential rise that was assigned to the appearance of the cation. The time constants for creation of the cation from the fits shown in Figure 5 were 22.3 ± 3.9, 26.5 ± 1.5 and 19.4 ± 0.8 ps for **3T**, **4T** and **5T**, respectively.

2T Fitting Procedure and Results. The combination of a much shorter excited state lifetime for the dye alone, the substantial spectral overlap between the excited state and the oxidized dye and the lack of a measured fluorescence decay lifetime of the dye alone precluded use of the above procedure to determine the electron transfer lifetime for **2T**. Instead, the excited state lifetime for the dye alone was evaluated by fitting the changes in the transient absorption at 2.46 eV using the sum of two exponential decays with time constants of 1.3 ± 0.3 and 7 ± 2 ps (Figure 6). Both time constants were substantially shorter that than those found for **3T**, **4T** and **5T**. The short lifetime for **2T** is consistent with previous reports of bithiophene lifetimes.[22, 23] Lap et al reported the lifetime of the excited state absorption being 50 ps,[22] whereas Prlj and coworkers performed a computational study of unsubstituted bithiophene and concluded that the S1 lifetime would be 1.8 ps, which agreed with the current study.[24]

Three exponential terms, two decays and one rise, were required to model the change in spectral intensity at 2.35 eV (Figure 6). The smallest time constant (1.2 ± 0.1 ps) corresponded to the early time feature in the dye-alone pump-probe spectrum. In the fit, the time constant of the second decay and the rise were required to be the same. The 36 ± 2 ps time constant was assigned to the excited state electron transfer resulting in the appearance of the oxidized dye.

Discussion

The conduction band minimum energy of 4.3 nm ZnO NCs was calculated using the values

for the change in the band gap as a function of size reported by Sarma and coworkers[25] and adding it to the bulk ZnO band gap and the work function measured on a nanocrystalline ZnO film.

The electronic structures of **2T**, **3T**, **4T** and **5T** were reported previously along with their lowest excited state energies in CH_2Cl_2.[6] In each of these molecules the LUMO orbital density was shown to be delocalized over the cyanoacrylic group and the adjacent thiophene unit. As this functionality is identical in each compound, there was little change in the energy of the LUMO among the dyes, a fact found to be consistent between the computational and experimental electrochemical measurements.[6]

Transient absorption of the excited states was examined using ultrafast pump-probe spectroscopy on solutions where the number of dyes per ZnO NC was kept low (~2:1) to minimize the impact of dye aggregation. At higher dye to NC ratios (~20:1), Stern Volmer experiments display behavior consistent with concentration quenching. Based on steady state spectroscopic measurements, the bands of the stimulated emission and ground state hole in the difference spectra were known. Figure 4 shows that all the compounds exhibit transient absorption bands in the visible-near IR region range corresponding to the excited state. The main excited state absorption band overlaps in all cases with the bleach in ground state absorption and the stimulated emission spectrum to some extent, which complicates the exact assignment of the absorption maximum. The energies of the main transient absorption bands agree with previous studies on extended thiophene oligomers that are unsubstituted, including the clear trend when going from two to five thiophenes where the excited state absorption band appears at lower energies.[22]

Measurement of the excited state decay of the free dyes was critical for comparison to the changes observed for the dye/ZnO NC dyads. Both the dye alone and the dye/NC systems exhibited multiphasic dynamics. The lifetimes observed for **3T**, **4T** and **5T** were similar to related

terthiophene-based dyes that did not have cyanoacrylate anchoring groups.[3, 5] The smallest dye, **2T**, exhibited much shorter lifetimes. When ZnO NCs were combined with the dyes in an approximate 2:1 dye to NC ratio, a distinct transient absorption was observed that corresponded closely to the absorption observed from chemical oxidation of the dye using nitrosonium ion. The appearance of this absorption was assigned to electron transfer from the excited state of the dye to the ZnO NC. The excited state electron transfer time constants (Table 1) decrease by a factor of ~2 from **2T** to **5T**.

Marcus theory of electron transfer to semiconductors is shown in eq. 2 where $\rho(E)$ is the density of acceptor states as a function of energy above the acceptor band edge, E, $f(E, E_F)$ is the Fermi occupancy factor (taken as zero for a wide gap semiconductor such as ZnO), $H(E)$ is the electronic coupling, λ is the reorganization energy, T is temperature (K) and ΔG_0 is the energy difference between the conduction band edge and the excited state of the bound dye.[26]

$$k_{ET} = \frac{2\pi}{\hbar}\int_{-\infty}^{+\infty} dE\rho(E)\left(1 - f(E, E_F)\right)\left|\overline{H(E)}\right|^2 \frac{1}{\sqrt{4\pi\lambda k_B T}} exp\left[\frac{(\lambda+\Delta G_0+E)^2}{4\lambda k_B T}\right] \quad (2)$$

Integration over E accounts for transfer into available conduction band states. Given the similarities in the LUMOs for all of the dyes, with the excited state charge density enhanced at the cyanoacrylate anchoring group, as well as the similarity in the link to the ZnO NCs, we anticipate that the electronic coupling, $H(E)$ will be essentially the same for all of the dye/ZnO NC dyads.

Addition of subsequent thiophene rings systematically reduces the energy of the absorption band primarily due to an increase in the energy of the HOMO.[6] The significant changes in the absorption energy across this series of compounds does not result in a significant change in the relative energies of the excited state relative to the ZnO NC conduction band. As shown in Table

1, the free energy change for electron transfer from the excited state of the dye to the conduction band of the ZnO NC, ΔG_o, for the dyes are within 0.09 eV of one another. In addition to the small differences in the driving force, the free energy changes ($\Delta G_o \sim$ -1 eV) exceeds our expectation for the reorganization energy, and is thus sufficiently large to provide access to barrierless ($\lambda + E = -\Delta G_0$) transfer in all cases, greatly reducing the dependence of the rate on the exponential term in eq. 2. Consistent with this, the electron transfer time constants decrease by less than a factor of two in going from **2T** to **5T**.

The small magnitude of this change is consistent with the expected small change in the density of acceptor states energetically coincident with barrierless transfer. A similar trend was reported in an earlier study using zinc porphyrins attached to ZnO NCs.[1] For the porphyrin/ZnO NCs, however, the excited state electron transfer lifetimes ranged from 245 – 369 ps; two orders of magnitude slower than those of the current study. While this is consistent with the lower value of ΔG_0 by 0.3-0.4V, the porphyrin measurements were conducted in methanol and the anchoring carboxylate group was separated from the porphyrin ring by a phenyl group. In addition, the porphyrin chromophore was attached to ZnO NCs capped with acetate rather than oleate as used in this study. The combination of these factors renders it difficult to assign the longer ET lifetime for the porphyrin system to any one factor.

Electron transfer lifetimes for two related terthiophene dyes that were anchored to the ZnO NCs via a carboxylate group connected directly to the terthiophene ring system, 3',4'-dibutyl-5"-phenyl-[2,2':5',2"-terthiophene]-5-carboxylate and 5"-hexyl-[2,2':5',2"-terthiophene]-5 carboxylate were 3.5 and 1.5 ps, respectively.[3, 5] Likewise, the terthiophene dye bound to ZnO NCs via a phosphonate ([2,2':5',2"-terthiophene]-5-phosphonate) had a shorter τ_{ET} (6.1 ps[5]) than any of the cyanoacrylate-bound dyes of the current study. While the ΔG_0 was larger by ~ 0.2V for

all three of these dyes, the solvent, NC capping group and the lack of a cyanovinyl linker also differed from the current study.

Extrapolating from isolated ZnO NCs to nanocrystalline films, this research suggests that one combine this homologous series of dyes (**2T - 5T**) on the same film in order to substantially broaden the light harvesting spectral coverage without impacting the electron transfer rates. The potential benefit derives from the increase in solar photons absorbed by the combination of dyes.

Conclusions

A series of known dyes comprising two to five thiophene units capped on one end with a cyanoacrylate group were anchored to well-defined, oleate-capped ZnO nanocrystals dispersed in dichloromethane. Fluorescence lifetimes of the ter-, quarter- and quinquethiophene dyes were 760, 1560 and 790 ps, respectively, but the fluorescence of the bithiophene dye was too weak for lifetime measurements. Stern Volmer experiments revealed a complex behavior consistent with previous studies demonstrating static quenching by the ZnO NCs and suggestive of concentration quenching at high dye to NC ratios. For dyads having dye to NC ratios near unity, ultrafast pump-probe spectroscopic measurements in the visible and near IR region showed instantaneous formation of the dye excited states, which rapidly decayed via electron transfer to the ZnO NC with concomitant formation of a longer-lived absorption assigned to the oxidized dye. The time constants for the excited state electron transfers were 36 ± 2, 22.3 ± 3.9, 26.5 ± 1.5 and 19.4 ± 0.8 ps for the bi, ter, quarter and quinquethiophene dyes, respectively. The small changes were attributed to two factors; first, the similarity in the energy of the LUMO of the four dyes, and second, the free energy change for the electron transfer was sufficiently large to push the reaction into the barrierless regime.

AUTHOR INFORMATION

Corresponding Authors

Wayne L. Gladfelter

*E-mail: wgl@umn.edu. Tel.: 612-624-4391

David A. Blank

*E-mail: blank@umn.edu. Tel.: 612-624-0571

ACKNOWLEDGEMENTS

This work is funded by a grant from the Chemical Sciences, Geosciences, and Biosciences Division, Office of Basic Energy Sciences, Office of Science, U.S. Department of Energy under Award Number DE-FG02-07ER15913.

REFERENCES

1. A. S. Huss, A. Bierbaum, R. Chitta, D. J. Ceckanowicz, K. R. Mann, W. L. Gladfelter and D. A. Blank, *J. Am. Chem. Soc.*, 2010, **132**, 13963-13965.
2. R. J. Hue, R. Vatassery, K. R. Mann and W. L. Gladfelter, *Dalton Trans.*, 2015, **44**, 4630-4639.
3. A. S. Huss, J. E. Rossini, D. J. Ceckanowicz, J. N. Bohnsack, K. R. Mann, W. L. Gladfelter and D. A. Blank, *J. Phys. Chem. C*, 2011, **115**, 2-10.
4. J. E. Rossini, A. S. Huss, J. N. Bohnsack, D. A. Blank, K. R. Mann and W. L. Gladfelter, *J. Phys. Chem. C*, 2011, **115**, 11-17.
5. A. N. Oehrlein, A. Sanchez-Diaz, P. C. Goff, G. M. Ziegler, T. M. Pappenfus, K. R. Mann, D. A. Blank and W. L. Gladfelter, *Phys. Chem. Chem. Phys.*, 2017, **19**, 24294-24303.
6. M. Planells, A. Abate, H. J. Snaith and N. Robertson, *ACS Appl. Mater. Interfac.*, 2014, **6**, 17226-17235.
7. N. A. Anderson, X. Ai, D. T. Chen, D. L. Mohler and T. Q. Lian, *J. Phys. Chem. B*, 2003, **107**, 14231-14239.

8. J. N. Clifford, E. Palomares, M. K. Nazeeruddin, M. Gratzel, J. Nelson, X. Li, N. J. Long and J. R. Durrant, *J. Am. Chem. Soc.*, 2004, **126**, 5225-5233.
9. E. Rohwer, I. Minda, G. Tauscher, C. Richter, H. Miura, D. Schlettwein and H. Schwoerer, *Chemphyschem*, 2015, **16**, 943-948.
10. J. Wiberg, T. Marinado, D. P. Hagberg, L. C. Sun, A. Hagfeldt and B. Albinsson, *J. Phys. Chem. B*, 2010, **114**, 14358-14363.
11. K. Hara, Y. Tachibana, Y. Ohga, A. Shinpo, S. Suga, K. Sayama, H. Sugihara and H. Arakawa, *Sol. Energy Mater. Sol. Cells*, 2003, **77**, 89-103.
12. K. Hara, Z. S. Wang, T. Sato, A. Furube, R. Katoh, H. Sugihara, Y. Dan-Oh, C. Kasada, A. Shinpo and S. Suga, *J. Phys. Chem. B*, 2005, **109**, 15476-15482.
13. Z. S. Wang, Y. Cui, K. Hara, Y. Dan-Oh, C. Kasada and A. Shinpo, *Adv. Mater.*, 2007, **19**, 1138-1141.
14. Y. Hu, A. Ivaturi, M. Planells, C. L. Boldrini, A. O. Biroli and N. Robertson, *J. Mater. Chem. A*, 2016, **4**, 2509-2516.
15. L. Zhang and J. M. Cole, *ACS Appl. Mater. Interfac.*, 2015, **7**, 3427-3455.
16. K. Prashanthan, T. Thivakarasarma, P. Ravirajan, M. Planells, N. Robertson and J. Nelson, *J Mater Chem C*, 2017, **5**, 11758-11762.
17. A. Abate, M. Planells, D. J. Hollman, S. D. Stranks, A. Petrozza, A. R. S. Kandada, Y. Vaynzof, S. K. Pathak, N. Robertson and H. J. Snaith, *Advanced Energy Materials*, 2014, **4**.
18. Y. Hu, A. Abate, Y. M. Cao, A. Ivaturi, S. M. Zakeeruddin, M. Gratzel and N. Robertson, *J. Phys. Chem. C*, 2016, **120**, 15027-15034.
19. D. A. Schwartz, N. S. Norberg, Q. P. Nguyen, J. M. Parker and D. R. Gamelin, *J. Am. Chem. Soc.*, 2003, **125**, 13205-13218.
20. A. S. Huss, T. Pappenfus, J. Bohnsack, M. Burand, K. R. Mann and D. A. Blank, *J. Phys. Chem. A*, 2009, **113**, 10202-10210.
21. R. Vatassery, J. A. Hinke, A. Sanchez-Diaz, R. Hue, K. R. Mann, D. A. Blank and W. L. Gladfelter, *J. Phys. Chem. C*, 2013, **117**, 10708-10715.
22. D. V. Lap, D. Grebner and S. Rentsch, *J. Phys. Chem. A*, 1997, **101**, 107-112.
23. D. Grebner, M. Helbig and S. Rentsch, *J. Phys. Chem.*, 1995, **99**, 16991-16998.
24. A. Prlj, B. F. E. Curchod and C. Corminboeuf, *Phys. Chem. Chem. Phys.*, 2015, **17**, 14719-14730.
25. R. Viswanatha, S. Sapra, B. Satpati, P. V. Satyam, B. N. Dev and D. D. Sarma, *J. Mater. Chem.*, 2004, **14**, 661-668.
26. N. A. Anderson and T. Lian, *Annu. Rev. Phys. Chem.*, 2005, **56**, 491-519.

1

Table 1. Factors contributing to the electron transfer lifetimes. Values for E_{HOMO}, E^{Opt}_{gap}, and E* were taken from the literature.[6] The values for CBE and E_{HOMO} are relative to vacuum.

Dye	Particle Size (nm)	CBE (eV)	E_{HOMO} S^+/S (V)	E^{Opt}_{gap} (eV)	E* (eV)	ΔG_o (eV)	ET time constant (ps)
2T	4.3	-4.09	-5.80	2.58	-3.22	0.76	36 ± 2
3T	4.3	-4.09	-5.54	2.31	-3.23	0.77	22.3 ± 3.9
4T	4.3	-4.09	-5.58	2.19	-3.19	0.81	26.5 ± 1.5
5T	4.3	-4.09	-5.27	2.12	-3.15	0.85	19.4 ± 0.8

FIGURE CAPTIONS

Figure 1. Molecular structure of **2T** (n = 1), **3T** (n = 2), **4T** (n = 3) and **5T** (n = 4).

Figure 2. Electronic adsorption (solid lines) and fluorescence spectra (dashed lines) of **2T, 3T, 4T and 5T** in CH_2Cl_2.

Figure 3. Stern-Volmer experiments for **3T, 4T, and 5T.** Each dye concentration is 1.8×10^{-5} M.

Figure 4. Ultrafast data for A) **2T** alone in CH_2Cl_2 B) 2:1 **2T** to ZnO C) **3T** alone in CH_2Cl_2 D) 2:1 **3T** to ZnO E) **4T** alone in CH_2Cl_2 F) 2:1 **4T** to ZnO G) **5T** alone in CH_2Cl_2 H) 2:1 **5T** to ZnO. Each color corresponds to the averaged ΔOD in the visible range for a selection on time delays between the pump and probe in picoseconds. The blank space around 1.55 eV is due to residual light from the fundamental in the continuum probe. For the oxidized dye absorption, peaks are shown only for the oxidized dye and any ground state dye absorption has been omitted.

Figure 5. Scaled transient absorption intensities of **3T**, **4T** and **5T** in CH_2Cl_2 solution with and without ZnO NCs.

Figure 6. Normalized transient absorption intensity of **2T** in CH_2Cl_2 solution pumped at 400 nm excitation. Vertical bar separates in lin-log time axis.

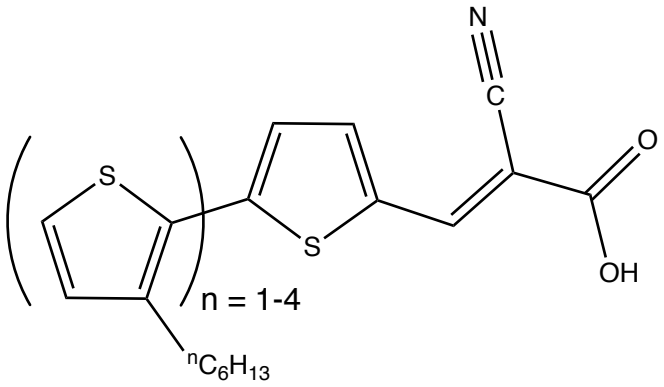

Figure 1. Molecular structures of **2T** (n = 1), **3T** (n = 2), **4T** (n = 3) and **5T** (n = 4).

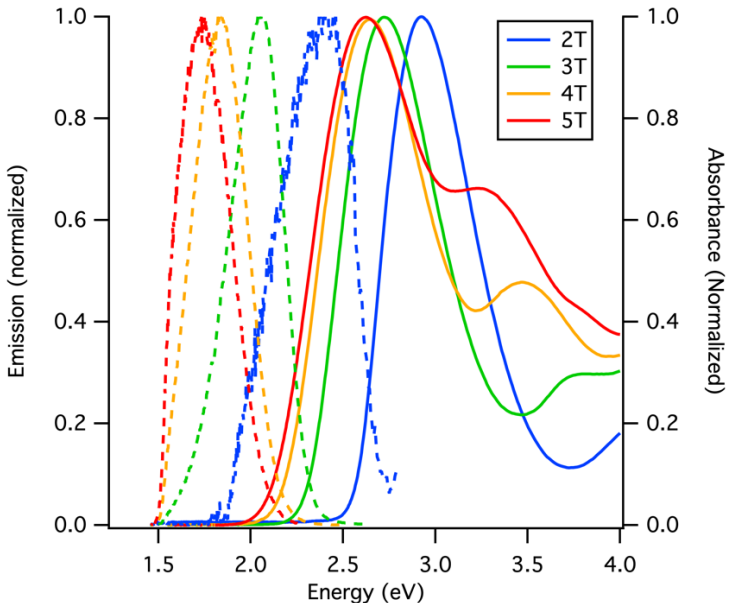

Figure 2. Electronic adsorption (solid lines) and fluorescence spectra (dashed lines) of **2T, 3T, 4T and 5T** in CH_2Cl_2.

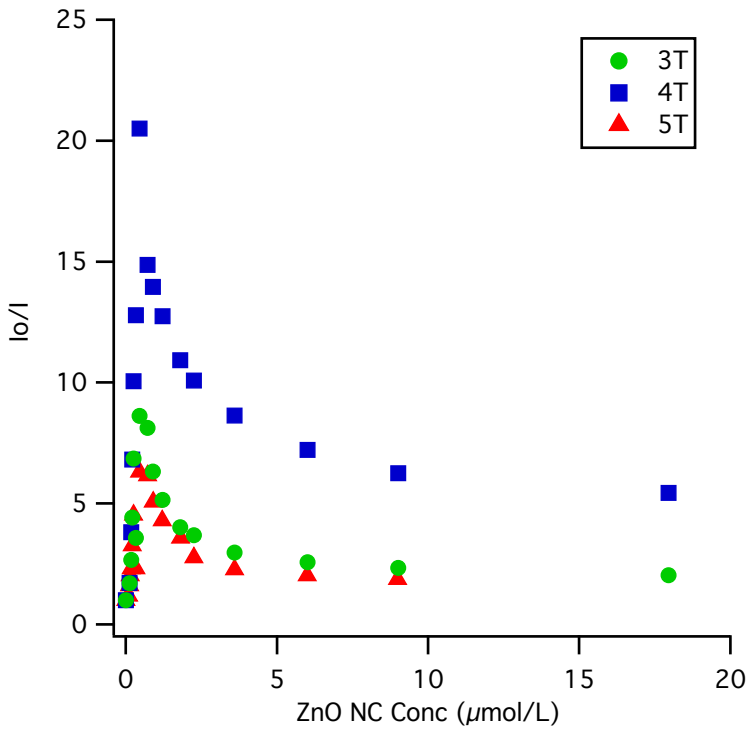

Figure 3. Stern-Volmer experiments for **3T, 4T, and 5T.** Each dye concentration is 1.8 x 10^{-5} M.

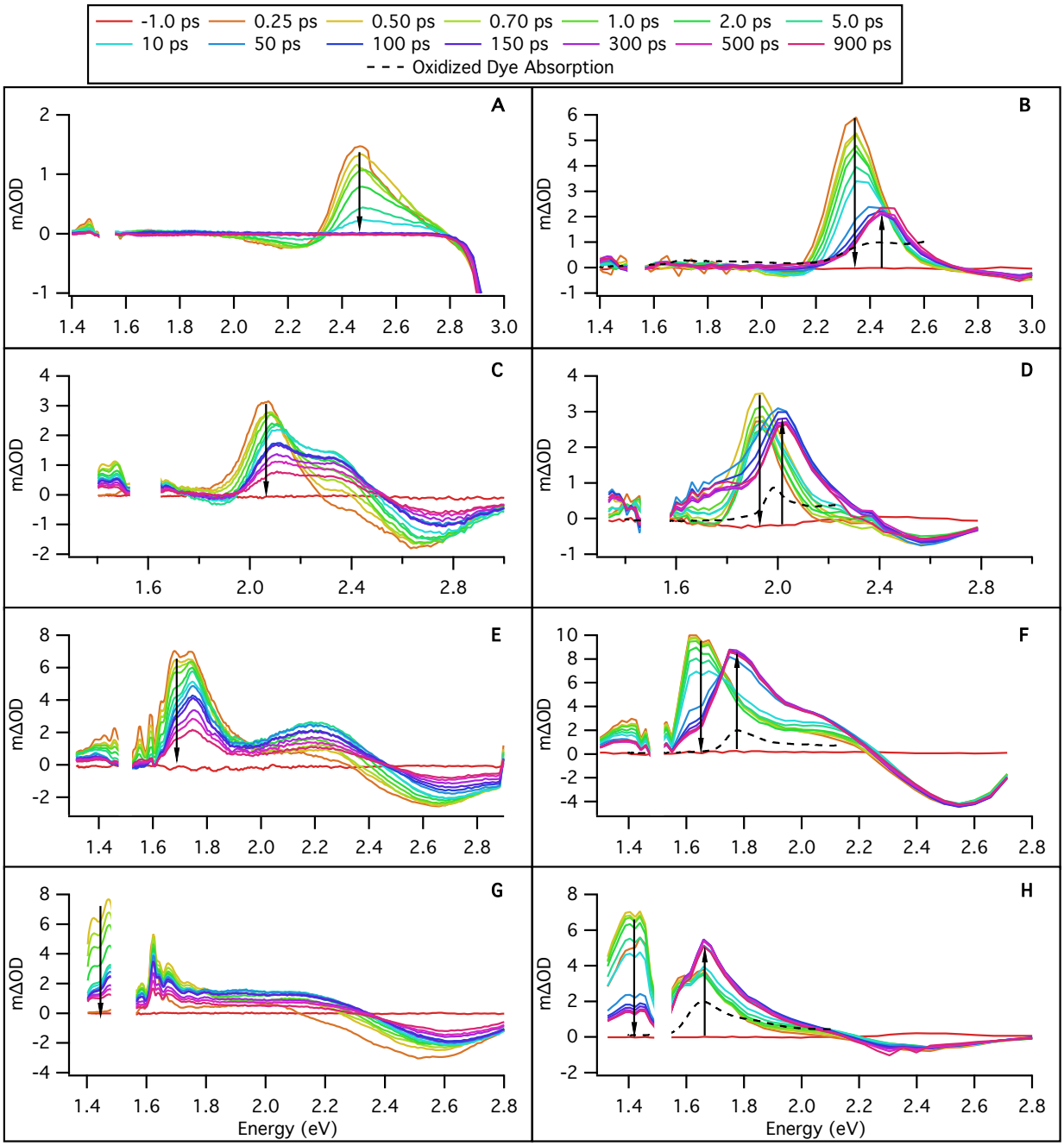

Figure 4. Ultrafast data for A) **2T** alone in CH_2Cl_2 B) 2:1 **2T** to ZnO C) **3T** alone in CH_2Cl_2 D) 2:1 **3T** to ZnO E) **4T** alone in CH_2Cl_2 F) 2:1 **4T** to ZnO G) **5T** alone in CH_2Cl_2 H) 2:1 **5T** to ZnO. Each color corresponds to the averaged ΔOD in the visible range for a selection on time delays between the pump and probe in picoseconds. The blank space around 1.55 eV is due to residual light from the fundamental in the continuum probe. For the oxidized dye absorption, peaks are shown only for the oxidized dye and any ground state dye absorption has been omitted.

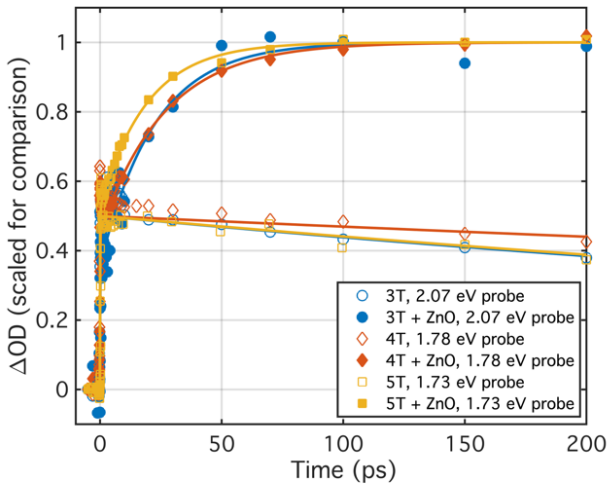

Figure 5. Scaled transient absorption intensities of **3T**, **4T** and **5T** in CH_2Cl_2 solution with and without ZnO NCs.

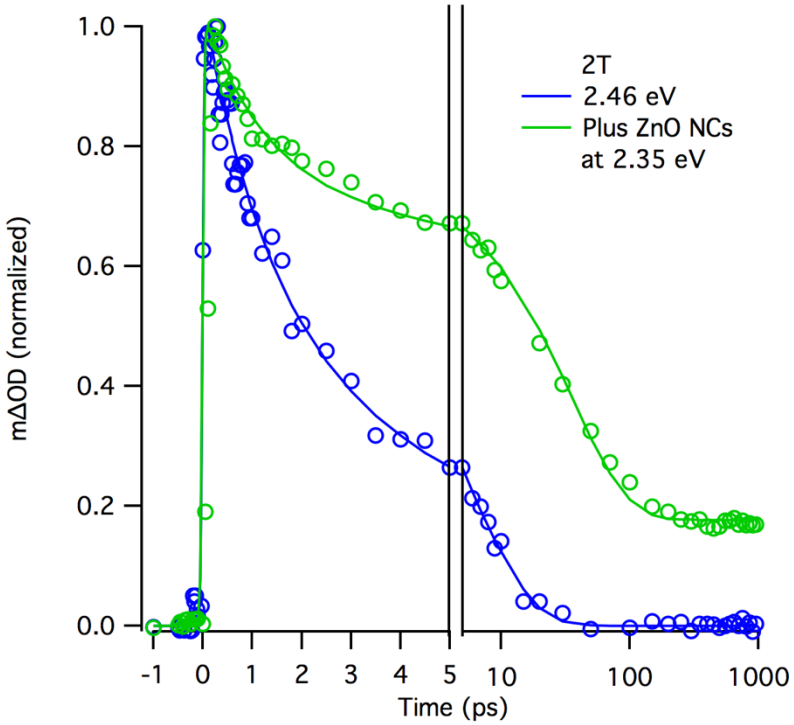

Figure 6. Normalized transient absorption intensity of **2T** in CH_2Cl_2 solution pumped at 400 nm excitation. Vertical bar separates in lin-log time axis.